IEEE Access
Multidisciplinary | Rapid Review | Open Access Journal

Received February 20, 2020, accepted March 12, 2020, date of publication March 17, 2020, date of current version April 6, 2020.

Digital Object Identifier 10.1109/ACCESS.2020.2981384

Dynamic Arc Current Distribution of Parallel Vacuum Arcs Subjected to Bipolar Axial Magnetic Field

HAOMIN LI, ZIHAN WANG, YINGSAN GENG, (Member, IEEE), ZHIYUAN LIU, (Member, IEEE), AND JIANHUA WANG, (Senior Member, IEEE)
State Key Laboratory of Electrical Insulation and Power Equipment, Xi'an Jiaotong University, Xi'an 710049, China

Corresponding author: Zihan Wang (zhwang92@163.com)

This work is supported by the National Natural Science Foundation of China under Grant 51937009.

ABSTRACT The objective of this paper is to determine dynamic anode and cathode arc current distribution of parallel vacuum arcs subjected to bipolar axial magnetic field. Drawn arc experiments were carried out in a demountable vacuum chamber. A split bipolar axial magnetic field electrode with diameter of 100 mm was specially designed. Arc current of two half split electrode discs were measured through Rogowski coils out of the vacuum chamber. Experimental current ranged from 4.5 to 45.0 kA. Vacuum arc behaviors were recorded by a high-speed camera. Unbalance phenomena of anode current and cathode current of parallel vacuum arcs were observed. The maximum average anode and cathode current density difference between parallel vacuum arcs at current of 45.0 kA were 2.57 and 2.52 A/mm^2, respectively. Critical value of both anode and cathode current difference ratio at time instant of maximum arc current difference with different arc initial conditions was 0.60. The maximum critical value of time instant of maximum anode and cathode current differences between parallel vacuum arcs with one strong arc branch at arc initial were 3.5 and 4.0 ms, respectively. Moreover, a three-interval arc current development model was proposed to describe unbalance phenomena of parallel vacuum arcs.

INDEX TERMS Parallel vacuum arcs, vacuum arc modes, axial magnetic field, arc current.

I. INTRODUCTION

Arc current is a key physical parameter of vacuum arcs. Anode current density is closely associated with anode energy flux density input and anode phenomena [1], [2]. Generally, anode serves as a passive collector of arc plasma when arc current density is relatively low (e.g., in the diffuse arc mode). As anode become active with high current density (e.g., in the footpoint mode and anode spot mode), anode begins to work as an arc plasma source. It is mainly because local molten area on anode surface caused by inhomogeneous energy flux density input would generate large quantity of metallic vapor from anode [3], [4]. Cathode current density represents electron, ion, and metallic vapor emitting during arcing. Cathode spots, which serve as main source of metallic vapor, sustain vacuum arcs during arc discharge [5]. For vacuum interrupter, severe anode and cathode surface erosion caused by high-current vacuum arcs have significant effect on its electrical lifetime, withstand voltage capability, and short-current interruption capability [6], [7].

Extensive efforts have been devoted to determine vacuum arc current distribution. By employing seven independent elements working as anode, anode current density in each element was determined [8]. The axial and radial anode current density in front of anode in diffuse arc mode was measured by means of a multiprobe and a diamagnetic loop, respectively [9]. A multiring anode setup was used to determine anode current density in diffuse arc mode [10]. The algebraic reconstruction technique algorithm was applied to estimate 2-D current density distribution in a moving arc root [11]. In [11], linear current distribution in a moving arc root along seven directions was measured though multiple split cathode with different slit angle setup. By means of 4-split anode electrode and Helmholtz coils, effect of axial magnetic field on current density in the central anode area was obtained [12]. Besides, contributions related to arc current

The associate editor coordinating the review of this manuscript and approving it for publication was Chenghong Gu.

This work is licensed under a Creative Commons Attribution 4.0 License. For more information, see https://creativecommons.org/licenses/by/4.0/

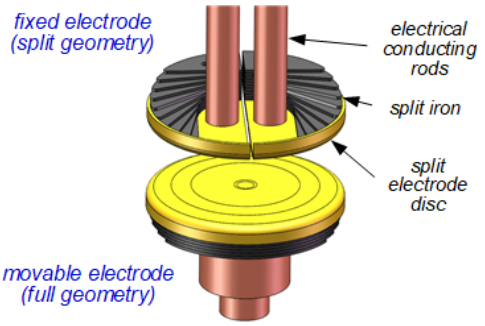

FIGURE 1. Split bipolar axial magnetic field electrode geometry.

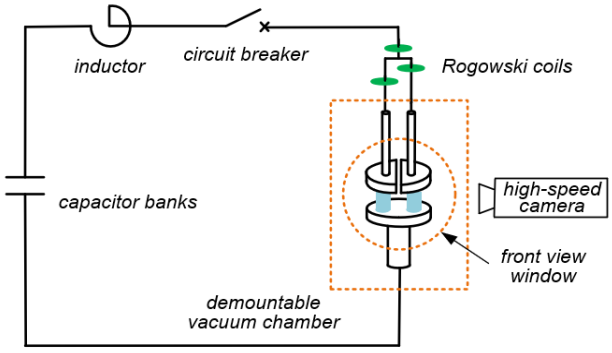

FIGURE 2. Arrangement of experimental circuit.

based on numerical calculation method were reported. References [13]–[15]. Most investigations mainly focus on anode and cathode arc current density of vacuum arcs with single arc column subjected to unipolar axial magnetic fields (AMF) or without magnetic field. However, arc current distribution of dual vacuum arcs in parallel are still not clear. In [16], experimental investigation was carried out of one electrical arc burning in the air connected to a vacuum arc in parallel. Whereas, arc characteristics of parallel vacuum arcs are quite different from characteristics of air arc and vacuum arc setup. In our previous investigations, non-synchronous arc phenomena in parallel vacuum arcs subjected to bipolar axial magnetic field have been qualitatively described [17], [18]. However, vacuum arc current in each parallel arc branch during arcing was not yet determined quantitively.

The objective of this paper is to determine dynamic anode and cathode arc current distribution of parallel vacuum arcs subjected to bipolar axial magnetic field. Split electrode setup was applied. Dynamic anode and cathode arc current of each parallel during arcing were measured. Relationships between arc current, maximum parallel arc current difference, and time instant of maximum parallel arc current difference were determined. The effect of vacuum arc initial condition on the parallel vacuum arc current different ratio was analyzed. Based on the experimental observation, a three-interval arc current development model of parallel vacuum arcs was proposed, which helped to reveal anode and cathode current dynamic distribution principles of parallel vacuum arcs.

II. EXPERIMENTAL SETUP

A. SPLIT ELECTRODE GEOMETRY

Fig. 1 shows split electrode geometry. An electrode disc with diameter of 100 mm was split into two half-moon shape pieces by a slit of 2 mm width, symmetrically. The martial of electrode disc was Cu50Cr50. Two electrical conducting rods in parallel connected to the two split electrode discs. A group of horseshoe shaped iron plates were set behind the electrode disc to collect induced magnetic field around two electrical conducting rods. The magnetic field was forced out of the iron plates into electrode gap region near the open slit of horseshoe shaped iron plates. Thus, a bipolar axial magnetic field was generated. Parallel vacuum arcs were formed due to the effect of the bipolar axial magnetic field. Parallel vacuum arc current could be measured by means of split electrode disc setup. For split electrode geometry, both iron plates and electrode disc were separated. Current in each electrical conducting rod could be regarded as the same value of arc current in the related split electrode disc.

B. EXPERIMENT CIRCUIT

Experimental circuit arrangement is shown in Fig. 2. Drawn arc experiments were carried out in a demountable vacuum chamber with a pressure of $\sim 10^{-4}$ Pa. In the experiment, split electrode was fixed to the vacuum chamber. A full horseshoe type electrode served as movable electrode driven by a spring actuator. Split electrode operated as anode and cathode, respectively. Opening velocity was 2.0 m/s. Sinusoidal current was generated by an *L-C* circuit with pre-charged capacitor banks. Arc current ranged from 4.5 to 45.0 kA. Arcing time with one current half-wave was 8.5 to 10.5 ms due to the mechanical dispersion of actuator. Vacuum arc behavior was obtained by a high-speed camera with recording speed of 2×10^4 fps and exposure time of 4 μs. The viewing angle was in parallel with electrode surface. Rogowski coils were set outside the vacuum chamber. Two Rogowski coils were used to measure current in each separated electrical conducting rod. The measured current was regarded as the arc current in parallel vacuum arcs. The total current in the experiment was recorded by another Rogowski coil.

III. EXPERIMENTAL RESULTS

A. UNBALANCE PHENOMENA OF PARALLEL VACUUM ARCS

Fig. 3 shows typical vacuum arc behavior of parallel vacuum arcs subjected to bipolar axial magnetic field. Arc duration was 20.7 ms with two current half-waves. Split electrode served as cathode in the first current half-wave with current of 15.4 kA. After first current zero, the polarity was reversed.

Split electrode worked as anode with current of 12.9 kA in the second current half-wave. Cathode and anode arc current of parallel vacuum arcs were measured in the same arc discharge process (in Fig. 3) is shown in Fig. 4. Fig. 4(a) illustrates the dynamic arc current in the left and right parallel arc branches during arcing. Meanwhile, total current of the

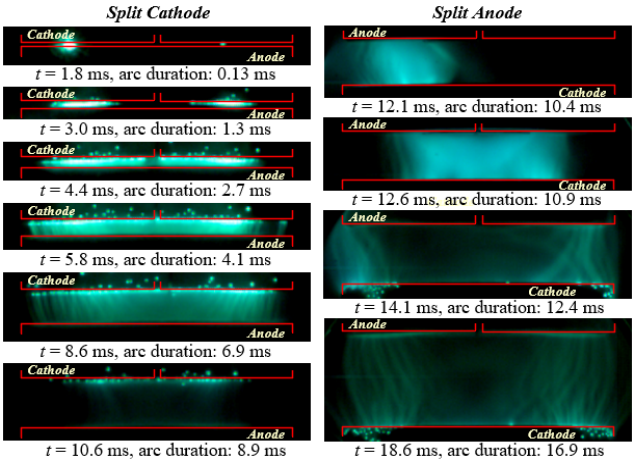

FIGURE 3. Typical arc behavior of parallel vacuum arcs. Split electrode worked as cathode with current of 15.4 kA in the first current half-wave. Split electrode worked as anode with current of 12.9 kA in the second current half-wave.

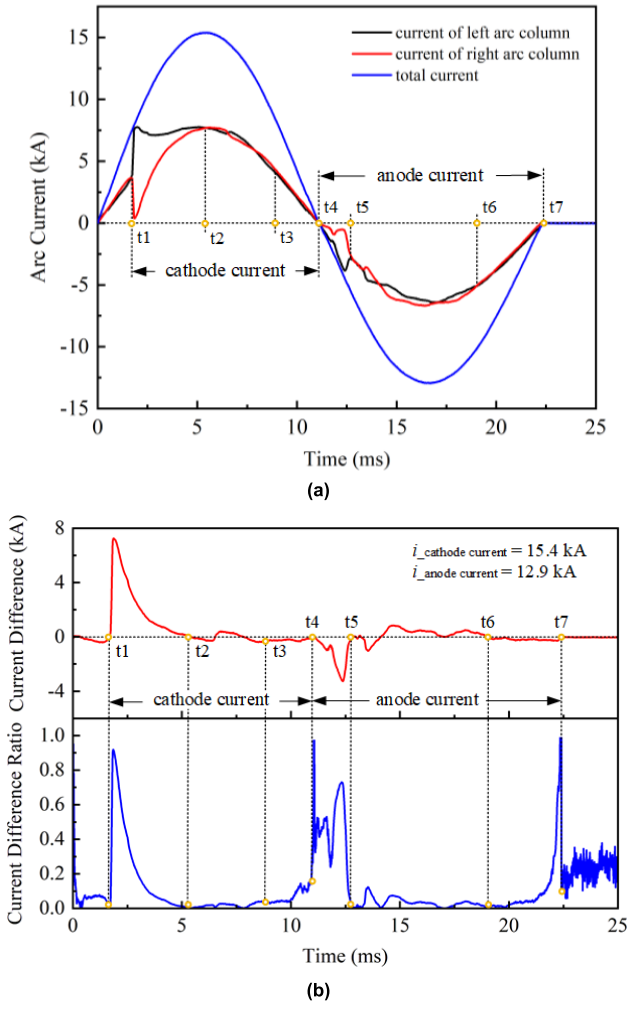

FIGURE 4. Dynamic cathode and anode arc current of parallel vacuum arcs. (a) Relationship between arc current of parallel arc branches and total arc current. (b) Cathode and anode current difference between twin parallel vacuum arcs.

parallel vacuum arcs was presented. Vacuum arcs ignited at both sides of the split electrode at time instant t1 of 1.7 ms after electrodes separation. At time instant of 1.8 ms, brighter arc appeared at the left side. While at the right side, only a weak luminous arc was observed. Cathode arc current of left and right arc branch was 7.6 and 0.4 kA, which indicated extremely unbalanced arc current after arc initial. As electrode gap increased, cathode spot moved from the arc initial position to the fringe of split electrode disc, as shown in the arc images at time instant of 3.0 and 4.4 ms in Fig. 3. Cathode arc current of left arc branch decreased at first. Then it slightly increased. Cathode arc current of right arc branch continuously increased. At time instant t2 of 5.4 ms, cathode spots distributed on the whole split electrode disc surface. Cathode arc current of left and right arc branch had appropriately the same value of 7.7 kA. From time instant t2 to t3 of 7.9 ms, cathode arc current of two parallel arc branches maintained at a relative balanced state with alternative higher current value. After t3, vacuum arc evolved into multi-cathode spot arc mode (in which mode cathode spots separated with independent plasma jet). Vacuum arcs were fully diffused. Cathode current of parallel vacuum arcs decreased with a relative same decreasing ratio.

First current zero appeared at time instant t4 of 11.1 ms. Vacuum arc reignited after t4. At time instant of 12.1 ms, vacuum arc was observed at left side. Then, vacuum arcs appeared on both sides at t5 of 12.6 ms. Between t4 and t5, vacuum arcs were unstable and shifted between left and right position due to the weak axial magnetic field. Arc currents of parallel arc branches were unbalanced. With the increase of arc current, two arc branches gradually separated. From t5 to t6 of 19.0 ms, parallel vacuum arcs were relative stable. Vacuum arcs became slightly distorted in the large electrode gap. After t6, vacuum arcs were in multi-cathode spot arc mode.

Fig. 4(b) shows dynamic arc current difference and dynamic arc current difference ratio between parallel vacuum arc branches. In order to estimate the unbalanced level arc current of parallel vacuum arcs, current difference ratio is defined. The current difference ratio of parallel vacuum arcs can be calculated by the current difference between parallel vacuum arcs divided by total arc current. It represents the level of unbalanced vacuum arc current. Higher current difference ratio indicates a larger current of one arc branch. According to Fig. 4(b), current difference reached the maximum value of 7.1 kA at 1.9 ms (electrode separated at 1.7 ms). The current difference ratio was 0.91. It rapidly decreased to 0.20 within 1.1 ms. At time instant t2, current difference ratio was zero. Afterwards, current difference ratio was below 0.05 which indicated balanced parallel vacuum arcs during this period. Near the time instant t4, current difference ratio was approximately 1 because of the large calculation error near current zero. Although the current difference ratio was high before current zero, it did not represent a large current difference value because arc current and arc energy input were low enough near current zero. After arc reigniting, the average value of current difference ratio between t4 and t5 was 0.50, which suggested unbalanced arc current process.

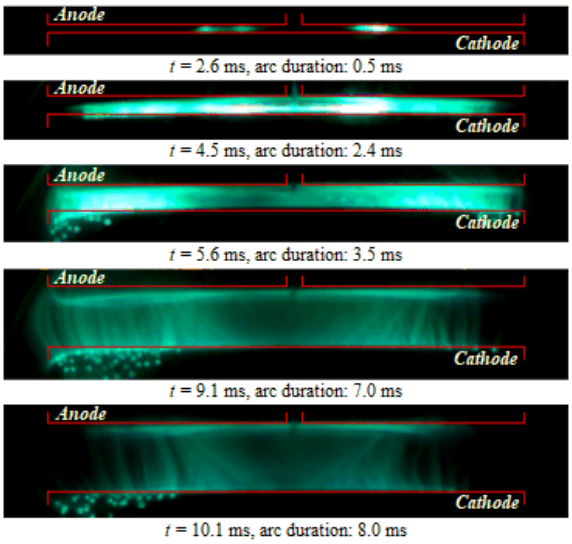

FIGURE 5. Arc behavior of parallel vacuum arcs. Split electrode worked as anode with current of 32.6 kA.

After time instant t5, the current difference ratio was below 0.12. At 0.5 ms before second current zero, current difference ratio increased sharply.

Based on the arc current characteristics of parallel vacuum arcs shown in Fig. 4, unbalance phenomena of parallel vacuum arc current were observed. Parallel cathode current difference ratio had a peak after electrode separation. It was probably affected by the vacuum arc initial condition, e.g., arc ignition position, arc phase, and electrode surface condition. The cathode current difference ratio decreased to below 0.12 after t2. It indicated that the cathode current difference maintained at a low level in the diffuse arc mode (in which mode arc plasma diffused and filled contact gap) with cathode spot distributing on the split electrode surface homogeneously.

B. ANODE CURRENT DISTRIBUTION OF PARALLEL VACUUM ARCS

1) DEVELOPMENT OF ANODE CURRENT DIFFERENCE

Vacuum arc behavior of parallel vacuum arcs at arc current of 32.6 kA is shown in Fig. 5. Split electrode worked as anode. Fig. 6 represents anode current of parallel vacuum arcs during arc discharge. Electrode separated at time instant A1 of 2.1 ms. In Fig. 5, vacuum arcs appeared at both sides of electrode near the center at 2.6 ms. Anode arc current in the left and right arc branches were 9.5 and 11.8 kA, respectively. In order to further describe the arc current variation of left and right arc branches, the minus sign before current difference ratio indicated a larger current in right arc branch in this paper. The current difference ratio at 2.6 ms was −0.13. From time instant A2 to A3 of 4.5 ms, vacuum arcs at both sides moved to the whole electrode surface. Parallel vacuum arcs were in the intense arc mode (in which mode distinct boundary of vacuum arc appeared under short contact gap). During this period, arc current in the left arc branch was higher than

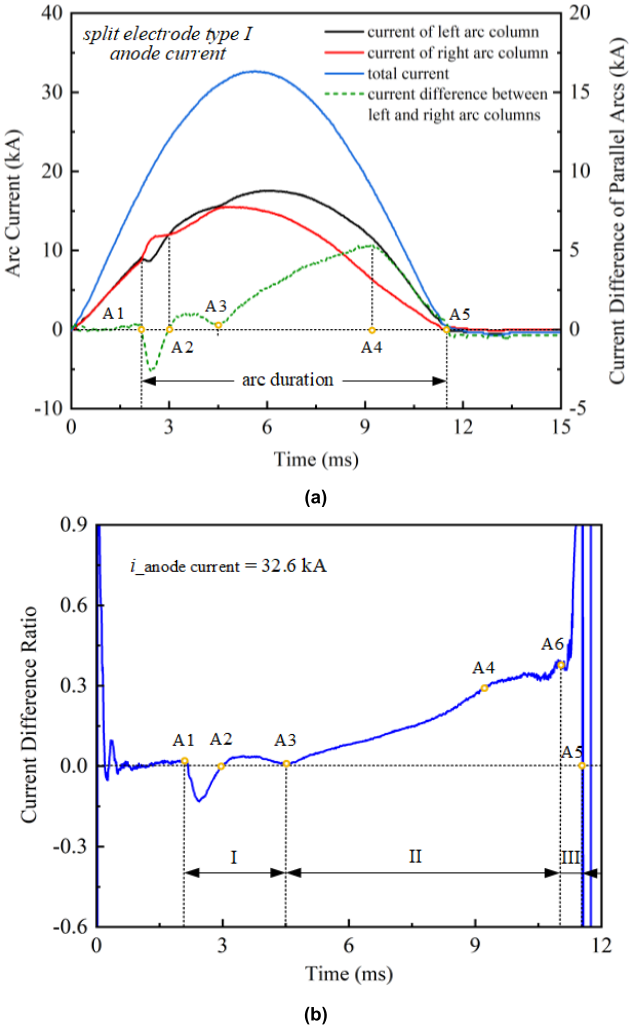

FIGURE 6. Dynamic anode arc current of parallel vacuum arcs. (a) Relationship between parallel anode arc current and total arc current. (b) Anode current difference between parallel vacuum arcs.

the current in the right arc branch. After 4.5 ms, parallel arc branches were observed. Arc current difference between left and right arc branches continuously increased to the maximum value of 4.8 kA at A4 of 9.2 ms. At this moment, arc current in the left and right arc branches were 11.4 and 6.6 kA, respectively. The current difference ratio was 0.31. After time instant A4, current difference between left and right arc branches was decreasing until current zero (A5). Parallel vacuum arcs during this period were fully diffused. Anode surface was becoming relative dark. Fig. 6(b) shows the anode current difference ratio with arc current of 32.6 kA. From time instant A1 to A3, anode current difference ratio oscillated with decay feature until parallel arc current tended to in balanced state. In order to describe this current self-balance process at arc initial, arc current self-balance time is defined. It is the time duration from electrode separation to arc current of two parallel arc branches reaching a relative balanced state. Arc current self-balance time indicates the self-balance capability of parallel vacuum arcs from the unbalanced arc initial. Generally, short arc current self-balance time is preferred to

avoid inhomogeneous parallel arc energy input which will result in severe erosion at one side of electrode disc. Anode arc current self-balance time with current of 32.6 kA was 2.4 ms. After time instant A3, parallel vacuum arc branches were formed. Anode current difference ratio increased from 0.01 to 0.30 at time instant A4 rapidly. Afterwards, anode current difference ratio increased to 0.38 at A6 gradually. During this period, anode current difference ratio continuously increased which indicated that parallel vacuum arcs tended to be more unbalanced. From A6 to current zero, arc current was lower than 4.0 kA. Parallel vacuum arcs were in multi-cathode spot arc mode. Large anode current difference ratio mainly caused by calculation error did not represented a large absolute value of arc current difference.

Based on the anode current difference ratio, anode current of parallel vacuum arcs during arc discharge could be divided into 3 intervals as shown in Fig. 6(b). Interval I was the arc initial period from time instant A1 to A3. Vacuum arcs were in the unstable movement stage in the interval I. During this period, vacuum arc ignited at random positions and then it moved to whole electrode surface. Anode parallel vacuum arcs current presented self-balance characteristics at arc initial until parallel vacuum arcs finally formed. Interval II was the stable arc burning period from time instant A3 to A6. Parallel vacuum arcs were in the relative stable burning stage. In this period, anode arc current of parallel vacuum arcs tended to become further unbalanced according to current difference ratio curve. It indicated that anode parallel arc current had an unbalance tendency in the stable arc burning period instead of self-balance characteristics at arc initial. Interval III was the arc decay period near current zero from time instant A6 to A5. During this period, vacuum arc was in multi-cathode spot arc mode with current below 5.0 kA typically. Because of continuously decreasing arc current, high current difference ratio in the arc decay period did not represent large current difference value actually. Interval III indicated the nonsynchronous cathode spots decay process of parallel vacuum arcs.

2) UNBALANCE CHARACTERISTICS OF ANODE CURRENT UNDER DIFFERENT CURRENT LEVELS

Anode current characteristics of parallel vacuum arcs were shown in Fig. 7. Split electrode served as anode with arc current ranged from 4.5 to 45.0 kA. In the experiment, three cases of vacuum arc behaviors at arc initial were observed, i.e., 1) two approximate balanced arcs at both sides of split electrode discs, 2) one strong arc branch and one weak arc branch at two split electrode discs, 3) only one strong arc branch appeared at one side of split electrode disc. Case 3) could be considered as an extreme condition of case 2). Therefore, two different arc initial conditions (case 1) and case 2)) were taken into consideration in the analysis of parallel anode current characteristics. Fig. 7(a) shows the relationship between total current and maximum anode current difference between parallel vacuum arcs. Vacuum arc with one strong arc branch at arc initial was observed when

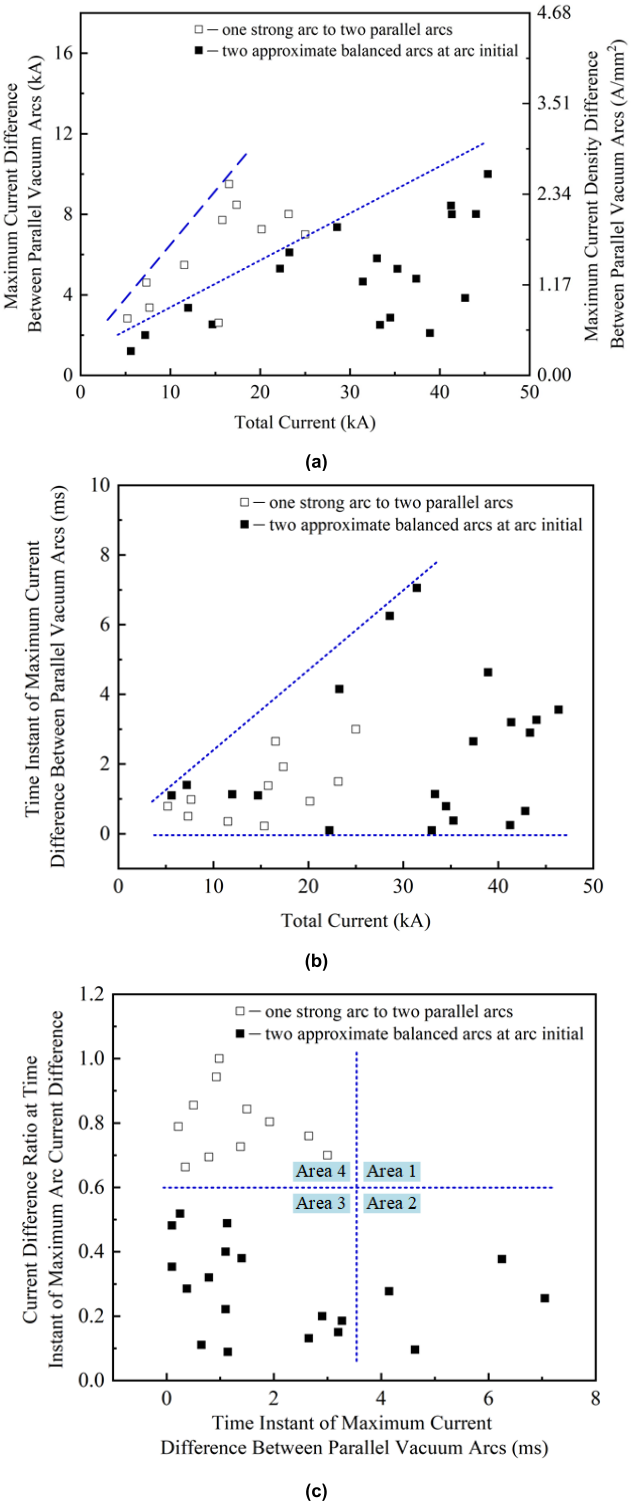

FIGURE 7. Anode current characteristics of parallel vacuum arcs with arc current ranged from 4.5 to 45.0 kA. (a) Relationship between total current and maximum anode current difference between parallel vacuum arcs. (b) Relationship between total current and time instant of maximum anode current difference between parallel vacuum arcs. (c) Relationship between current difference ratio and time instant of maximum anode current difference between parallel vacuum arcs.

current was lower than 25.0 kA. For a specific total current, the maximum anode current difference of arc initial case 1)

was larger than arc initial case 2). It suggested that one strong arc branch at arc initial was not preferred because it would lead to severe local electrode erosion caused by large anode current. The maximum anode current difference between parallel vacuum arcs with one strong arc branch at arc initial and with two approximate balanced arcs at arc initial could be estimated by equation (1) and (2), respectively

$$i_{a\_max\_diff} = 0.53 i_{total} + 1.14 \quad (1)$$

$$i_{a\_max\_diff} = 0.24 i_{total} + 0.77 \quad (2)$$

where $i_{a\_max\_diff}$ was the maximum anode current difference between parallel vacuum arcs, i_{total} was the total current of parallel vacuum arcs. According to equation (1) and (2), when total current was 40.0 kA, $i_{a\_max\_diff}$ with one strong arc branch at arc initial was 22.3 kA, which was 2.2 times higher than $i_{a\_max\_diff}$ with two approximate balanced arcs at arc initial. Besides, average current density is defined, which can be calculated through arc current divided by the area of split electrode disc. The maximum average anode current density difference between parallel vacuum arcs at current of 45.0 kA was 2.57 A/mm^2.

Fig. 7(b) shows the relationship between total current i_{total} and time instant of maximum anode current difference between parallel vacuum arcs $t_{a\_max\_diff}$. Vacuum arcs ignited at time instant zero. Time instant of maximum anode current difference between parallel vacuum arcs in the experiments were scattered in an open triangular region. With the increasing of total current, the dispersity of time instant of maximum anode current difference between parallel vacuum arcs was larger. When total current i_{total} was 10.0, 20.0, and 30.0 kA, the $t_{a\_max\_diff}$ was within 2.4, 4.7, and 6.9 ms, respectively.

Fig. 7(c) shows the relationship between time instant of maximum anode current difference between parallel vacuum arcs $t_{a\_max\_diff}$ and anode current difference ratio at time of maximum anode arc current difference $k_{a\_max\_diff}$ Four areas were divided based on crossing lines $t_{a\_max\_diff} = 3.5$ ms and $k_{a\_max\_diff} = 0.60$. When two approximate balanced arcs appeared at arc initial, the current difference ratio at time instant of maximum anode arc current difference in the experiments were scattered in the area 2 and area 3 with $k_{a\_max\_diff}$ lower than 0.60. If one strong arc branch was formed at arc initial, the current difference ratio at time instant of maximum anode arc current difference in the experiments only distributed in the area 4 with $k_{a\_max\_diff}$ higher than 0.60. Therefore, 0.60 would be regarded as the critical value of $k_{a\_max\_diff}$ with different arc initial conditions.

When one strong arc branch appeared at arc initial, ta_max_diff was shorter than 3.5 ms. It suggested that the maximum anode current difference between parallel vacuum arcs generally appeared in the interval I in the Fig. 6(b) due to the extreme unbalanced arc current at arc initial. The time instant of maximum anode current difference between parallel vacuum arcs ranged from 0.1 to 7.0 ms if two approximate balanced arcs appeared at arc initial. Thus, 3.5 ms could be considered as the maximum critical value of ta_max_diff for

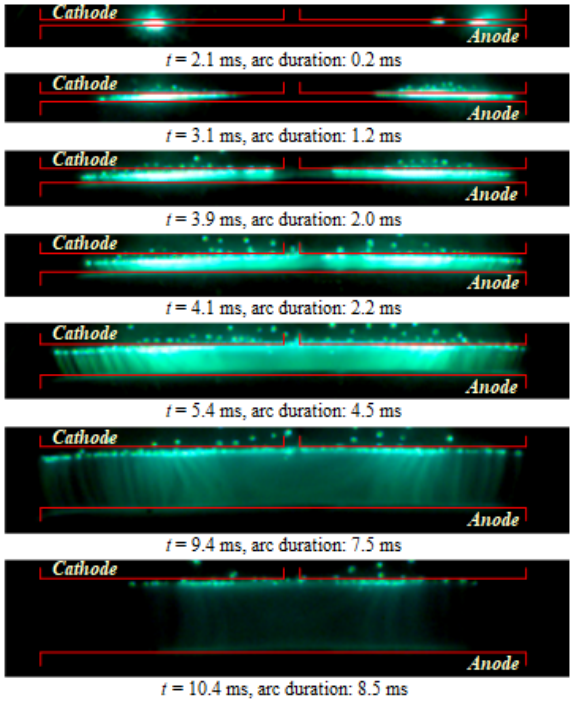

FIGURE 8. Arc behavior of parallel vacuum arcs. Split electrode worked as cathode with current of 18.9 kA.

the initial arc condition with one strong arc branch. According to the analysis above, it indicated that parallel vacuum arc behavior at arc initial had significant effect on the unbalance characteristics of parallel anode arc current.

C. CATHODE CURRENT DISTRIBUTION OF PARALLEL VACUUM ARCS

1) DEVELOPMENT OF CATHODE CURRENT DIFFERENCE

As the main plasma source during arc discharge, cathode played a different role from anode. In order to investigate cathode arc current distribution of parallel vacuum arcs, split electrode was set as cathode. Arc current ranged from 6.0 to 41.0 kA. Fig. 8 shows behavior of parallel vacuum arcs with arc current of 18.9 kA. Related parallel cathode arc current was measured as shown in Fig. 9. Electrode separated at time instant B1 of 1.9 ms. At 2.1 ms, two approximate balanced arcs appeared at both sides of split electrode. Cathode current of left and right arc branches was 6.2 and 5.1 kA, respectively. Cathode current difference and cathode current different ratio were 1.1 kA and 0.10. At time instant B2 of 3.1 ms, cathode current of parallel vacuum arc branches were in the same value of 1.4 kA. Between B1 and B2, cathode spots of each arc branch moved to the fringe of split electrode discs. Vacuum arcs were in the intense arc mode. From time instant B2 to B3 of 4.1 ms, cathode spots of parallel vacuum arcs tended to distribute on the entire electrode disc surface. Cathode current of left branch was higher than the current of right branch. Cathode current difference between left and right arc branch increased to 0.8 kA. The related cathode current difference ratio increased to 0.04 at B3. After B3,

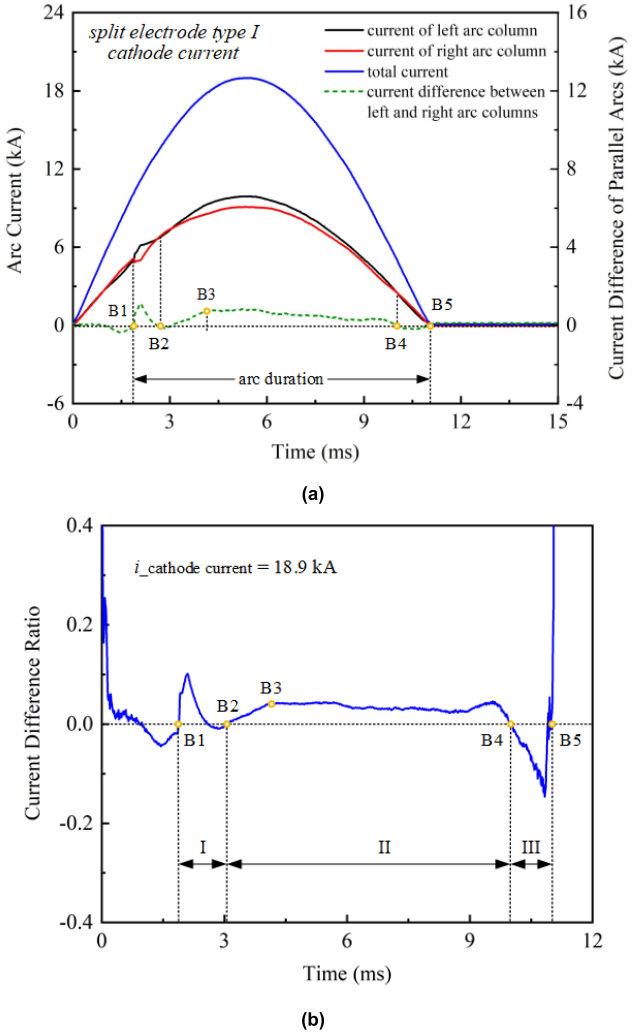

FIGURE 9. Dynamic cathode arc current of parallel vacuum arcs. (a) Relationship between parallel cathode arc current and total arc current. (b) Cathode current difference between parallel vacuum arcs.

cathode current difference between parallel arc branches decreased slightly due to the different current phase. The cathode current difference ratio remained almost the same value which indicated a quite stable arc period. Vacuum arcs were in diffuse arc mode. Near time instant B4 of 9.9 ms, arc current was 5.2 kA. From time instant B4 to current zero (B5), vacuum arcs were in the multi-cathode arc mode with cathode current difference lower than 0.2 kA.

During arc discharge, cathode current of parallel vacuum arcs could be divided into 3 intervals based on the cathode current difference ratio as shown in Fig. 9(b). The classification standard of 3 intervals was similar to the parallel anode current. Interval I was the arc initial period from time instant B1 to A2. It was the self-balance period of parallel vacuum arcs. The cathode current self-balance time at current of 18.9 kA was 1.2 ms. Interval II was the stable arc burning period from time instant B2 to B4. Cathode current difference ratio was relative stable when cathode spots spread over the whole split electrode surface in the diffuse arc mode. Interval III was the arc decay period with low arc current

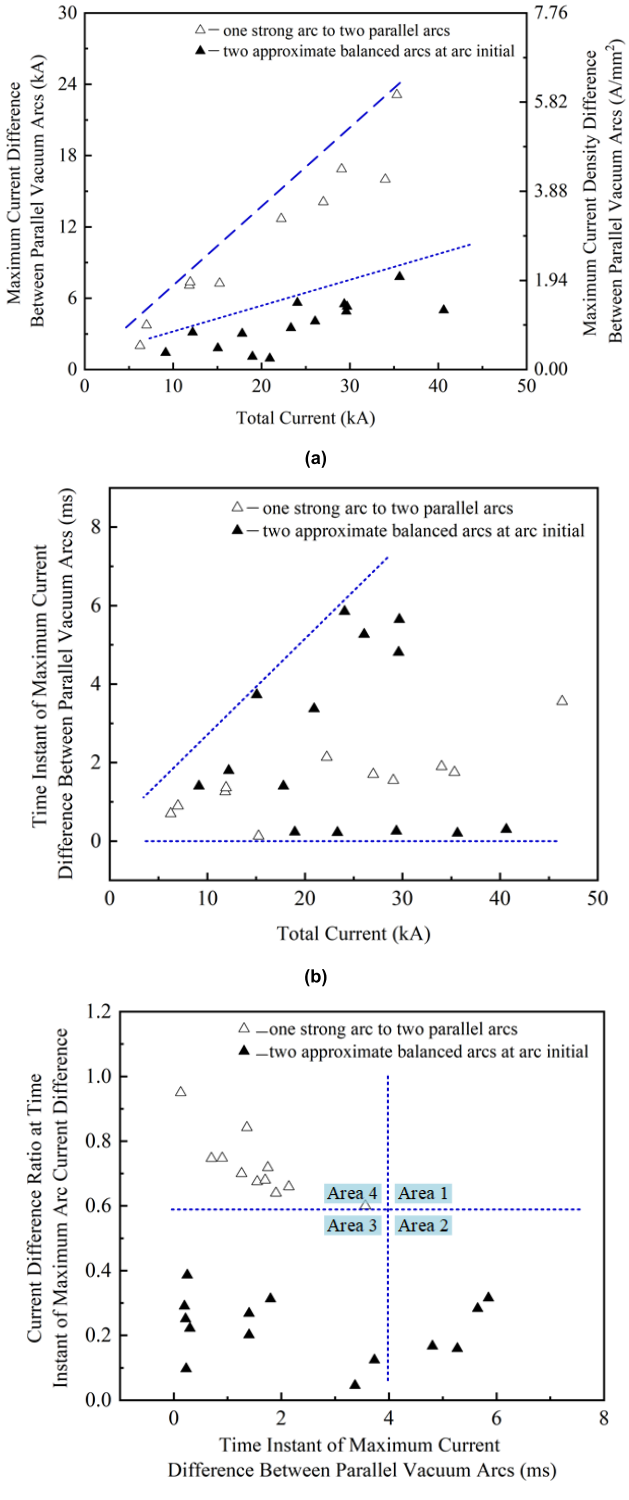

FIGURE 10. Cathode current characteristics of parallel vacuum arcs with arc current ranged from 6.0 to 41.0 kA. (a) Relationship between total current and maximum cathode current difference between parallel vacuum arcs. (b) Relationship between total current and time instant of maximum cathode current difference between parallel vacuum arcs. (c) Relationship between current difference ratio and time instant of maximum cathode current difference between parallel vacuum arcs.

near current zero. High cathode current difference ratio in this period is mainly due to calculation error near current zero.

Cathode current characteristics of parallel vacuum arcs were shown in Fig. 10. Fig. 10(a) shows the relationship between total current and maximum cathode current difference between parallel vacuum arcs. Vacuum arc with one strong arc branch at arc initial was observed with current lower than 35.0 kA. Compared with maximum anode current difference with arc initial of one strong arc branch, the maximum cathode current difference with arc initial of two approximate balanced arcs at both sides of split electrode discs was higher for a specific total current. The maximum cathode current difference between parallel vacuum arcs with one strong arc branch at arc initial and with two approximate balanced arcs at arc initial could be estimated by equation (3) and (4), respectively

$$i_{c\_max\_diff} = 0.67 i_{total} + 0.03 \quad (3)$$

$$i_{c\_max\_diff} = 0.23 i_{total} + 0.74 \quad (4)$$

where $i_{c\_max\_diff}$ was the maximum cathode current difference between parallel vacuum arcs, i_{total} was total current of parallel vacuum arcs. According to equation (3) and (4), when total current was 20.0 kA, $i_{c\_max\_diff}$ with one strong arc branch and two approximate balanced arcs at arc initial was 13.4 kA and 5.3 kA. With total current increased to 40.0 kA, $i_{c\_max\_diff}$ with one strong arc branch at arc initial was 26.8 kA, which was 2.7 times higher than $i_{c\_max\_diff}$ with two approximate balanced arcs at arc initial. The maximum cathode average current density difference between parallel vacuum arcs at current of 40.0 kA was 2.52 A/mm^2.

2) UNBALANCE CHARACTERISTICS OF CATHODE CURRENT UNDER DIFFERENT CURRENT LEVELS

Fig. 10(b) shows the relationship between total current i_{total} and time instant of maximum cathode current difference between parallel vacuum arcs $t_{c\_max\_diff}$. Time instant of maximum cathode current difference between parallel vacuum arcs were scattered in an open triangular region. With the increasing of total current, time instant of maximum cathode current difference between parallel vacuum arcs had large dispersity. When total current i_{total} was 10.0, 20.0, and 30.0 kA, the $t_{c\_max\_diff}$ was within 2.7, 4.5, and 6.6 ms, respectively.

Fig. 10(c) shows the relationship between time instant of maximum cathode current difference between parallel vacuum arcs $t_{c\_max\_diff}$ and cathode current difference ratio at time instant of maximum cathode arc current difference $k_{c\_max\_diff}$. Four areas could be divided based on crossing lines $t_{c\_max\_diff} = 4.0$ ms and $k_{c\_max\_diff} = 0.60$. When two approximate balanced arcs appeared at arc initial, the current difference ratio at time instant of maximum cathode arc current difference in the experiments distributed in the area 2 and area 3 with $k_{c\_max\_diff}$ lower than 0.60. In the situation of one strong arc branch was formed at arc initial, the current difference ratio at time instant of maximum cathode arc current difference distributed in the area 4 with $k_{c\_max\_diff}$ higher than 0.60. Thus, the critical value of $k_{c\_max\_diff}$ with two kinds of arc initial conditions could be determined as 0.60. When one strong arc branch appeared at arc initial, t_{max_diff} was shorter than 4.0 ms. The time instant of maximum cathode current difference between parallel vacuum arcs ranged from 0.1 to 6.0 ms when two approximate balanced arcs appeared at arc initial. Here, 4.0 ms could be considered as the maximum critical value of $t_{c\_max\_diff}$ with one strong arc branch at arc initial.

IV. DISCUSSION

Unbalance phenomena of parallel vacuum arc current were observed. In the experiments, parallel arc current distribution for both anode and cathode had some common characteristics during arc discharge. In order to describe dynamic anode and cathode arc current development process, a three-interval arc current development model of parallel vacuum arcs was proposed according to current difference ratio of parallel vacuum arcs. Interval I was arc current self-balance period at arc initial. During this period, vacuum arcs expanded from arc ignition position to whole electrode surface. Self-balance feature of parallel anode and cathode arc current appeared in the interval I as shown in Fig. 6(b) and Fig. 9(b). For parallel vacuum arcs, three cases of vacuum arc behaviors at arc initial were observed in the experiment. Cathode spots were split to form new cathode spots rapidly and they were driven to move to the fringe of electrode disc by electromagnetic force. Unstable vacuum arcs were in expanded duration to form parallel arc branches. Current difference ratio curve decreased with fluctuation until parallel arc current tended to in balanced state. The typical during of interval I was within 4.5 ms. Interval II was stable arc burning period. Parallel vacuum arc branches existed in the period. Anode and cathode current difference ratio curves were quite different. Anode current difference ratio of parallel vacuum arcs continuously increased as shown in Fig. 6(b), which indicated an unbalance tendency in the interval II. Parallel current unbalance process might be affected by two factors, electrode surface condition after interval I and cathode phenomena in interval II. Generally, intense arc mode appeared in the interval I, which would lead to severe electrode erosion especially with large current. Due to different arc initial cases of parallel vacuum arcs, anode surface condition in two parallel arcing regions were different. The anode region with higher local temperature became more active. It had high probability to emit metallic vapor from anode, which was preferred to generate more of plasma in the relative arc branch by ionization. Thus, macro-current difference of two arc branches was observed. Besides, vacuum arcs in the interval II were mainly in the diffuse arc mode, during which cathodic vapor was the main contribution to arc plasma. Therefore, anode current could be influenced by cathode phenomena. Cathode current difference ratio of parallel vacuum arcs was relative stable in the diffuse arc mode as shown in Fig. 9(b), which indicated a relative balanced period in the interval II. In this period, independent cathode spots distributed on the entire split electrode disc surface homogeneously. Therefore, the cathode current difference ratio of parallel vacuum arcs

maintained at a relatively low stable value in the interval II. The typical during of interval II began after interval I and ended at 1.5 ms before current zero. Interval III was the arc decay period shortly before current zero with typical arc current lower than 5.0 kA. In this period, vacuum arcs were in the multi-cathode spot arc mode. Current difference ratio indicated nonsynchronous cathode spots decay process of parallel vacuum arcs. The three-interval arc current development model described the unbalance phenomena of parallel vacuum arcs from the angle of dynamic arc current distribution quantitively. Besides, unbalanced parallel vacuum arcs subjected to bipolar axial magnetic field would result in asymmetrical electrode erosion characteristics in parallel arcing region, e.g., molten layer depth, alloy content, surface microstructure [19]. In addition, arc current had influence on vacuum arc mode transition of parallel vacuum arc branches and the diameter of vacuum arc columns [17]. All these contributions help to better understand the unbalance phenomena of parallel vacuum arcs.

Parallel arc current of another split electrode geometry with split electrode disc and a complete horseshoe shaped iron plates was reported in [20]. Parallel arc current self-balance phenomena were observed during whole arcing discharge because of the function of complete iron plates connecting to two split electrode disc. The measured current of split electrode with complete iron plates were the current of parallel arc current affected by current sharing effect caused by complete iron plates. However, the split electrode applied in this paper had both split electrode disc and split horseshoe shaped iron plates. Two parts of split electrode were totally separated. Compared with measurement results in [20], the current measurement in this paper could be regarded as the current of related parallel arc branch.

V. SUMMARY

This paper experimentally determined dynamic anode and cathode arc current distribution of parallel vacuum arcs subjected to bipolar axial magnetic field. The conclusions are the following:

1) Unbalance phenomena of anode current and cathode current of parallel vacuum arcs were observed. Three-interval arc current development model was proposed to describe unbalance phenomena of parallel vacuum arcs. Interval I was the parallel arc current self-balance period at arc initial. During interval II, parallel anode and cathode arc current in the diffuse arc mode presented unbalance tendency and relative balanced characteristics, respectively. Interval III was the arc decay period shortly before current zero.

2) The maximum average anode current density difference between parallel vacuum arcs at current of 45.0 kA was 2.57 A/mm^2. The critical value of anode current difference ratio at time instant of maximum anode arc current difference with different arc initial conditions was 0.60. The maximum critical value of time instant of maximum anode current difference between parallel vacuum arcs with one strong arc branch at arc initial was 3.5 ms.

3) The maximum average cathode current density difference between parallel vacuum arcs at arc current of 45.0 kA was 2.52 A/mm^2. The critical value of cathode current difference ratio at time instant of maximum cathode arc current difference with different arc initial conditions was 0.60. The maximum critical value at time instant of maximum cathode arc current difference between parallel vacuum arcs with one strong arc branch at arc initial was 4.0 ms.

REFERENCES

[1] P. G. Slade, *The Vacuum Interrupter Theory, Design, and Application*. Boca Raton, FL, USA: CRC Press, 2008.
[2] H. C. Miller, "Anode modes in vacuum arcs: Update," *IEEE Trans. Plasma Sci.*, vol. 45, no. 8, pp. 2366–2374, Aug. 2017.
[3] S. Jia, Z. Shi, and L. Wang, "Vacuum arc under axial magnetic field: Experimental and simulation research," *J. Phys. D, appl. Phys.*, vol. 47, no. 40, Oct. 2014.
[4] A. Khakpour, S. Popov, S. Franke, R. Kozakov, R. Methling, D. Uhrlandt, and S. Gortschakow, "Determination of CR density after current zero in a high-current vacuum arc considering anode plume," *IEEE Trans. Plasma Sci.*, vol. 45, no. 8, pp. 2108–2114, Aug. 2017.
[5] B. Jüttner, "Cathode spots of electric arcs," *J. Phys. D, Appl. Phys.*, vol. 34, no. 17, pp. 103–123, Sep. 2001.
[6] G. A. Farrall, "Recovery of dielectric strength after current interruption in vacuum," *IEEE Trans. Plasma Sci.*, vol. PS-6, no. 4, pp. 360–369, Dec. 1978.
[7] H. Schellekens and M. B. Schulman, "Contact temperature and erosion in high-current diffuse vacuum arcs on axial magnetic field contacts," *IEEE Trans. Plasma Sci.*, vol. 29, no. 3, pp. 452–461, Jun. 2001.
[8] G. R. Mitchell, "High-current vacuum arcs—Part I: An experimental study," *Proc. Inst. Elect. Eng.*, vol. 117, no. 12, pp. 2315–2326, Dec. 1970.
[9] H. Schellekens, "A current distribution phenomenon in high-current vacuum arcs," *Phys. B C*, vol. 104, nos. 1–2, pp. 130–136, 1981.
[10] M. G. Drouet, P. Poissard, and J.-L. Meunier, "Measurement of the current distribution at the anode in a low-current vacuum arc," *IEEE Trans. Plasma Sci.*, vol. PS-15, no. 5, pp. 506–509, Oct. 1987.
[11] T. Xu, M. Rong, Y. Wu, Q. Ma, and X. Wang, "The estimation of the current-density distribution in a moving arc root using the ART algorithm," *IEEE Trans. Plasma Sci.*, vol. 37, no. 7, pp. 1311–1317, Jul. 2009.
[12] H. Ma, Y. Geng, Z. Liu, J. Wang, Z. Wang, and Z. Zhang, "Effect of an axial magnetic field and arc current on the anode current density in diffuse vacuum arcs," *Phys. Plasmas*, vol. 23, no. 9, Sep. 2016, Art. no. 093507.
[13] M. Nagashima, K. Yogi, T. Tsuji, E. Kaneko, N. Ide, and S. Yanabu, "Numerical calculation of current density distribution in a vacuum arc," in *Proc. Int. Symp. Discharges Electr. Insul. Vac.*, Matsue, Japan, Sep. 2006, pp. 415–418.
[14] M. Keidar, I. Beilis, R. L. Boxman, and S. Goldsmith, "2D expansion of the low-density interelectrode vacuum arc plasma jet in an axial magnetic field," *J. Phys. D, Appl. Phys.*, vol. 29, no. 7, pp. 1973–1983, Jul. 1996.
[15] L. Wang, S. Jia, Y. Liu, B. Chen, D. Yang, and Z. Shi, "Modeling and simulation of anode melting pool flow under the action of high-current vacuum arc," *J. Appl. Phys.*, vol. 107, no. 11, Jun. 2010, Art. no. 113306.
[16] A. Klajn, H. Markiewicz, and I. Surowka, "Experimental analysis of a vacuum arc connected parallel to an arc in air," in *Proc. 20th Int. Symp. Discharges Electr. Insul. Vac.*, Tours, France, 2002, pp. 407–410.
[17] H. Li, Z. Wang, Y. Geng, J. Wang, and Z. Liu, "High-current vacuum arc mode transition of a horseshoe-type axial magnetic field contact with long contact gap," *IEEE Trans. Plasma Sci.*, vol. 45, no. 8, pp. 2164–2171, Aug. 2017.
[18] H. Li, Z. Wang, Y. Geng, Z. Liu, and J. Wang, "Arcing contact gap of a 126-kV horseshoe-type bipolar axial magnetic field vacuum interrupters," *IEEE Trans. Plasma Sci.*, vol. 46, no. 10, pp. 3713–3721, Oct. 2018.
[19] Z. Wang, H. Li, Y. Li, S. Liu, J. Wang, Y. Geng, and Z. Liu, "Erosion characteristics of bipolar axial magnetic field contact exposed to high current vacuum arcs," in *Proc. 28th Int. Symp. Discharges Electr. Insul. Vac. (ISDEIV)*, Greifswald, Germany, Sep. 2018, pp. 299–302.
[20] H. Li, Z. Wang, S. Liu, Y. Geng, Z. Liu, J. Wang, and D. Uhrlandt, "Current balance characteristics of twin vacuum arc columns of horseshoe-type electrode," in *Proc. 28th Int. Symp. Discharges Electr. Insul. Vac. (ISDEIV)*, Greifswald, Germany, Sep. 2018, pp. 291–294.

HAOMIN LI was born in Henan, China, in 1988. He received the B.S. degree in electrical engineering from Xi'an Jiaotong University, Xi'an, China, in 2011, and the M.S. degree in electrical engineering from the Shenyang University of Technology, Shenyang, China, in 2014. He is currently pursuing the Ph.D. degree with the State Key Laboratory of Electrical Insulation and Power Equipment, Department of Electrical Engineering, Xi'an Jiaotong University.

His current research interests include spectroscopy and vacuum arc plasmas and their application.

ZIHAN WANG was born in Shaanxi, China, in 1992. He received the B.S. degree in electrical engineering from Xi'an Jiaotong University, Xi'an, China, in 2015, where he is currently pursuing the Ph.D. degree with the State Key Laboratory of Electrical Insulation and Power Equipment, Department of Electrical Engineering.

His research interests include vacuum arcs and optimization design of high-voltage vacuum interrupters.

YINGSAN GENG (Member, IEEE) was born in Henan, China, in 1963. He received the B.S., M.S., and Ph.D. degrees in electrical engineering from Xi'an Jiaotong University, China, in 1984, 1987, and 1997, respectively.

He is currently a Professor, the Deputy Director of the State Key Laboratory of Electrical Insulation and Power Equipment, and the Director of the Department of Electrical Apparatus, Xi'an Jiaotong University. His research interests include theory and application of low-voltage circuit breaker and high-voltage vacuum circuit breakers.

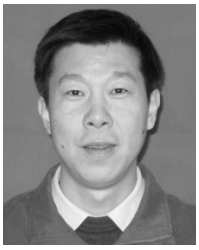

ZHIYUAN LIU (Member, IEEE) was born in Shenyang, China, in 1971. He received the B.S. and M.S. degrees in electrical engineering from the Shenyang University of Technology, Liaoning, China, in 1994 and 1997, respectively, and the Ph.D. degree in electrical engineering from Xi'an Jiaotong University, Xi'an, China, in 2001.

From 2001 to 2002, he was with the Research and Development Center, General Electric Company, Shanghai, China. Since 2003, he has been with the State Key Laboratory of Electrical Insulation and Power Equipment, Xi'an Jiaotong University. His current research interests include vacuum discharge, and vacuum arcs and their application. He is a Senior Member of the Current Zero Club and a member of the CIGRE Working Group A3.27.

JIANHUA WANG (Senior Member, IEEE) received the M.S. and Ph.D. degrees in electrical engineering from Xi'an Jiaotong University, China, in 1981 and 1985, respectively.

He is currently a Professor and the Director of the State Key Laboratory of Electrical Insulation and Power Equipment, Xi'an Jiaotong University. His research interests include theory and application of intelligent electrical apparatus systems and CAD/CAE in electrical engineering. He is the Chairman of the Professional Branch Committee on Intelligent Electrical System and its Applications of China Electro-Technical Society.